

See discussions, stats, and author profiles for this publication at: <https://www.researchgate.net/publication/277551383>

Magnetic interpretation using 3- D analytic signal

Article in *Geophysics* · January 1992

DOI: 10.1190/1.1443174

CITATIONS

804

READS

2,666

3 authors, including:



Joyce Verhoef

SOMT University of Physiotherapy

29 PUBLICATIONS 1,907 CITATIONS

[SEE PROFILE](#)



Mark Pilkington

Natural Resources Canada

138 PUBLICATIONS 5,436 CITATIONS

[SEE PROFILE](#)

Magnetic interpretation using the 3-D analytic signal

Walter R. Roest*, Jacob Verhoef‡, and Mark Pilkington*

ABSTRACT

A new method for magnetic interpretation has been developed based on the generalization of the analytic signal concept to three dimensions. The absolute value of the analytic signal is defined as the square root of the squared sum of the vertical and the two horizontal derivatives of the magnetic field. This signal exhibits maxima over magnetization contrasts, independent of the ambient magnetic field and source magnetization directions. Locations of these maxima thus determine the outlines of magnetic sources. Under the assumption that the anomalies are caused by vertical contacts, the analytic signal is used to estimate depth using a simple amplitude half-width rule. Two examples are shown of the application of the method. In the first example, the analytic signal highlights a circular feature beneath Lake Huron that has been identified as a possible impact crater. The second example illustrates the continuation of terranes across the Cabot Strait between Cape Breton and Newfoundland in eastern Canada.

INTRODUCTION

In recent years a large number of digital magnetic data sets covering different geological provinces has become available (cf. Dods et al., 1985; Committee for the Magnetic Anomaly Map of North America, 1988). The interpretation of magnetic anomalies over these large regions is facilitated by the development of special techniques for the statistical analysis of magnetic anomalies. Due to the much larger variation in crustal magnetic susceptibility, when compared with crustal density variations, and due to the existence of magnetic annihilators, i.e., magnetization distributions that do not lead to magnetic anomalies, some of the techniques used for the analysis of gravity data are not readily applicable to magnetic anomalies. Moreover, the interpretation of ob-

served magnetic anomalies is often complicated by the horizontal displacement of the anomalies with respect to their sources. This displacement, or skewness, results from the fact that the directions of the geomagnetic field and magnetization are, in general, not vertical.

Several methods have been developed that provide the depth to magnetic sources, the magnetization of the source material, and/or the geometry of the causative bodies. Of course, all methods suffer from the fact that no unique magnetization distribution can be found for a given set of observations. Nevertheless, a number of approaches have been successful in predicting source characteristics, using certain assumptions. Semiautomatic methods for analyzing profile data have been outlined by Nabighian (1972, 1974), Atchuta Rao et al. (1981), Thompson (1982), and Nelson (1988b). Other authors give a three-dimensional (3-D) treatment of the problem, suitable for use on gridded data sets (Nabighian, 1984; Blakely and Simpson, 1986; Nelson, 1988a; Reid et al., 1990; Wang and Hansen, 1990).

Most methods assume knowledge of the orientation of the present day magnetic field and of the source body magnetization. The inclination and declination of the present day magnetic field are well known. In the absence of oriented magnetic samples, one often assumes that the source body magnetization is purely induced; an assumption that is very often not justified. Here, we discuss the theory and application of the analytic signal—or energy envelope—of magnetic anomalies in 3-D proposed by Nabighian (1984). The advantage of the use of the absolute value of the analytical signal, originally developed for profile data by Nabighian (1972, 1974) (see also Atchuta Rao et al., 1981), is that its shape over linear structures is independent of the earth's magnetic field parameters and of the direction of magnetization of the source material. Therefore, the use of the absolute value of the analytic signal results in the determination of source characteristics without making assumptions on the direction of source body magnetization. This can be very important, especially in areas where the contribution of remanent magnetization to the observed anomalies is not known. We

Manuscript received by the Editor February 21, 1991; revised manuscript received July 2, 1991.

*Geophysics Division, Geological Survey of Canada, 1 Observatory Crescent, Ottawa, Ontario, K1A 0Y3 Canada.

‡Atlantic Geoscience Centre, Geological Survey of Canada, Bedford Institute of Oceanography, P. O. Box 1006, Dartmouth, Nova Scotia, B2Y 4A2 Canada.

© 1992 Society of Exploration Geophysicists. All rights reserved.

developed practical applications of the analytic signal that can be used to estimate source characteristics such as geometry and depth.

The method will be demonstrated with two examples taken from the Canadian aeromagnetic data base. The first example shows further evidence for a recently discovered circular feature, interpreted as a possible impact crater (Forsyth et al., 1990), beneath Lake Huron, on the border between Canada and the United States. The other example shows the continuation of structures between Newfoundland and Cape Breton Island in eastern Canada.

THEORY OF THE ANALYTIC SIGNAL IN 3-D

The analytic signal is most easily derived in the wavenumber domain, since it involves the calculation of derivatives of magnetic anomalies. The following convention is used for the forward and inverse 2-D Fourier transform $F[]$:

$$\begin{aligned} g(k_x, k_y) &= F[f(x, y)] \\ &= \int_{-\infty}^{\infty} \int_{-\infty}^{\infty} f(x, y) e^{-i(k_x x + k_y y)} dx dy \\ f(x, y) &= F^{-1}[g(k_x, k_y)] \\ &= \frac{1}{4\pi^2} \int_{-\infty}^{\infty} \int_{-\infty}^{\infty} g(k_x, k_y) e^{i(k_x x + k_y y)} dk_x dk_y, \end{aligned} \quad (1)$$

with k_x and k_y the wavenumbers in x and y directions. Using equation (1), wavenumber domain relations can be derived between the Fourier transforms of a magnetic anomaly M and of its horizontal and vertical derivatives, as well as relations between the different derivatives of a potential field anomaly (e.g., Nabighian, 1972, 1984; Nelson, 1988a; Pedersen, 1989).

Defining \hat{x} , \hat{y} , and \hat{z} as unit vectors in x , y , and z directions, respectively, allows the 3-D analytic signal of a potential field anomaly M to be written as:

$$\mathbf{A}(x, y) = \left(\frac{\partial M}{\partial x} \hat{x} + \frac{\partial M}{\partial y} \hat{y} + i \frac{\partial M}{\partial z} \hat{z} \right). \quad (2)$$

Equation (2) satisfies the basic requirement of the analytic signal (Nabighian, 1972, 1984), that its real and imaginary parts form a Hilbert transform pair. This can be illustrated by transforming equation (2) into the frequency domain and expressing it in terms of the gradient of the Fourier transform of the magnetic field:

$$\hat{i} \cdot F[\mathbf{A}(x, y)] = \hat{h} \cdot \nabla F[M] + i \hat{z} \cdot \nabla F[M], \quad (3)$$

where ∇ is the gradient operator in the frequency domain ($ik_x \hat{x} + ik_y \hat{y} + |k| \hat{z}$); $\hat{i} = \hat{x} + \hat{y} + \hat{z}$ and $\hat{h} = \hat{x} + \hat{y}$. The real part of equation (3) is formed by the horizontal derivative of the anomaly; the imaginary by its vertical derivative. Using a relation between the horizontal and vertical gradient of potential fields (Pedersen, 1989), it follows that

$$\begin{aligned} \hat{h} \cdot \nabla F[M] &= i \hat{h} \cdot \mathbf{k} F[M] = i \frac{(\hat{h} \cdot \mathbf{k})}{|\mathbf{k}|} |\mathbf{k}| F[M] \\ &= i \frac{(\hat{h} \cdot \mathbf{k})}{|\mathbf{k}|} \hat{z} \cdot \nabla F[M] \end{aligned} \quad (4)$$

that is, the horizontal and vertical derivatives of the magnetic anomaly are related by the 3-D Hilbert transform operator $i(\hat{h} \cdot \mathbf{k})/|\mathbf{k}|$ in the frequency domain. Equation (3) is therefore equivalent to the scalar equation (17) of Nabighian (1984) and represents a means of calculating the vertical derivative when horizontal derivatives in two perpendicular directions are available.

Of greater interest with respect to the automatic interpretation of gridded data is the 3-D equivalent of the 2-D amplitude function, or absolute value introduced by Nabighian (1972, 1974). From equation (2) it follows that the amplitude function is given by:

$$|\mathbf{A}(x, y)| = \sqrt{\left(\frac{\partial M}{\partial x} \right)^2 + \left(\frac{\partial M}{\partial y} \right)^2 + \left(\frac{\partial M}{\partial z} \right)^2}. \quad (5)$$

At this point, we would like to stress that this definition of the amplitude of the analytic signal is different from that of Ofoegbu and Mohan (1990, equation 7). They used a scalar addition of the two horizontal derivatives rather than a vector addition. The scalar addition was actually implicitly suggested in Nabighian's (1984) expression for the generalized analytic signal. However, it is clear that a scalar addition of two horizontal derivatives leads to a function that is sensitive to a rotation of the coordinate system. In practice, this results in an emphasis on structures that are parallel to the orientation of the chosen x - and y -axes, as can be observed in the example given by Ofoegbu and Mohan (1990).

The derivation of the amplitude of the analytic signal is outlined in Figure 1, which shows the magnetic anomaly over a square prism that is magnetized in an arbitrary direction. Next, the two horizontal and the vertical derivatives were calculated (Figure 1). The amplitude of the analytic signal was then obtained from equation (5), resulting in a function that shows maxima over the edges of the prism. It is well known that the shape of the absolute value of the analytic signal of magnetic anomalies over dikes and contrasts is independent of the directions of magnetization and of the earth's field (cf. Nabighian, 1972; Atchuta Rao et al., 1981). To prove that this is true for any 2-D anomaly, regardless of its source, we consider the case where $\partial M / \partial y = 0$, and find for the 2-D analytic signal:

$$\begin{aligned} F[\mathbf{A}(x)] &= \left(1 + \frac{|k_x|}{k_x} \right) F \left[\frac{\partial M(x)}{\partial x} \right] \\ &= i(k_x + |k_x|) F[M(x)] \\ &= \begin{cases} 2ik_x F[M(x)] & k_x > 0 \\ 0 & k_x \leq 0. \end{cases} \end{aligned} \quad (6)$$

Using this expression, we can derive the relation between the analytic signal of an anomaly observed at the magnetic pole and that of an anomaly observed at a location where the directions of the earth's magnetic field and of the magnetization are not vertical. Application of the inverse Fourier transform to equation (6) leads to the following expression for the analytic signal of a given anomaly M_{pole} , observed at the pole:

$$A_{\text{pole}}(x) = \frac{2i}{2\pi} \int_0^\infty k_x F[M_{\text{pole}}(x)] e^{ik_x x} dk_x. \quad (7)$$

Magnetic anomalies observed at the pole are related to those observed at a different location by the reduction to the pole operator:

$$F[M_{\text{pole}}(x, y)] = M_{\text{pole}}(k_x, k_y) = \left[\frac{|\mathbf{k}|^2}{(\mathbf{G} \cdot \mathbf{B}_0)(\mathbf{G} \cdot \mathbf{M}_0)} \right] M(k_x, k_y), \quad (8)$$

with $\mathbf{G} = (ik_x, ik_y, \mathbf{k})$, $\mathbf{B}_0 = (\alpha_x, \alpha_y, \alpha_z)$ and $\mathbf{M}_0 = (\ell_x, \ell_y, \ell_z)$ are the cosines of the present field and the source body magnetization, respectively. Using equation (8) with $k_y = 0$ because the anomaly is 2-D, and combining it with equation (7) leads to the following expression for the analytic signal of an anomaly not observed at the pole:

$$A(x) = \frac{2i}{2\pi} \int_0^\infty k_x \frac{(\mathbf{G} \cdot \mathbf{B}_0)(\mathbf{G} \cdot \mathbf{M}_0)}{k_x^2} M_{\text{pole}}(k_x) e^{ik_x x} dk_x = (i\alpha_x - \alpha_z)(i\ell_x - \ell_z) A_{\text{pole}}(x). \quad (9)$$

Assuming that the directions of the magnetization and of the earth's magnetic field are constant over the area, the direc-

tional cosines of the present field and the magnetization for a 2-D body can be written as:

$$\alpha_x = \left(\frac{\sin I_r}{\sin I'_p} \right) \cos I_r \quad \alpha_z = \left(\frac{\sin I_r}{\sin I'_p} \right) \sin I_r \quad (10)$$

$$\beta_x = \left(\frac{\sin I_p}{\sin I'_p} \right) \cos I_p \quad \beta_z = \left(\frac{\sin I_p}{\sin I'_p} \right) \sin I_p,$$

with I'_p and I_r the effective present field and source body magnetization inclinations, respectively. The effective inclination is the inclination projected perpendicular to the strike of the body α (α measured relative the magnetic north), i.e., $\tan I' = \tan I / \sin \alpha$. Finally, this yields for the absolute value of the analytic signal:

$$|A(x)| = \left(\frac{\sin I_p}{\sin I'_p} \right) \left(\frac{\sin I_r}{\sin I'_r} \right) |A_{\text{pole}}(x)| = C_p |A_{\text{pole}}(x)|. \quad (11)$$

Equation (11) shows that the shape of the absolute value of the analytic signal for 2-D bodies does not depend on the ambient magnetic field and source body magnetization parameters, or skewness of the anomaly. It should be noted again that the derivation of equation (11) is independent of

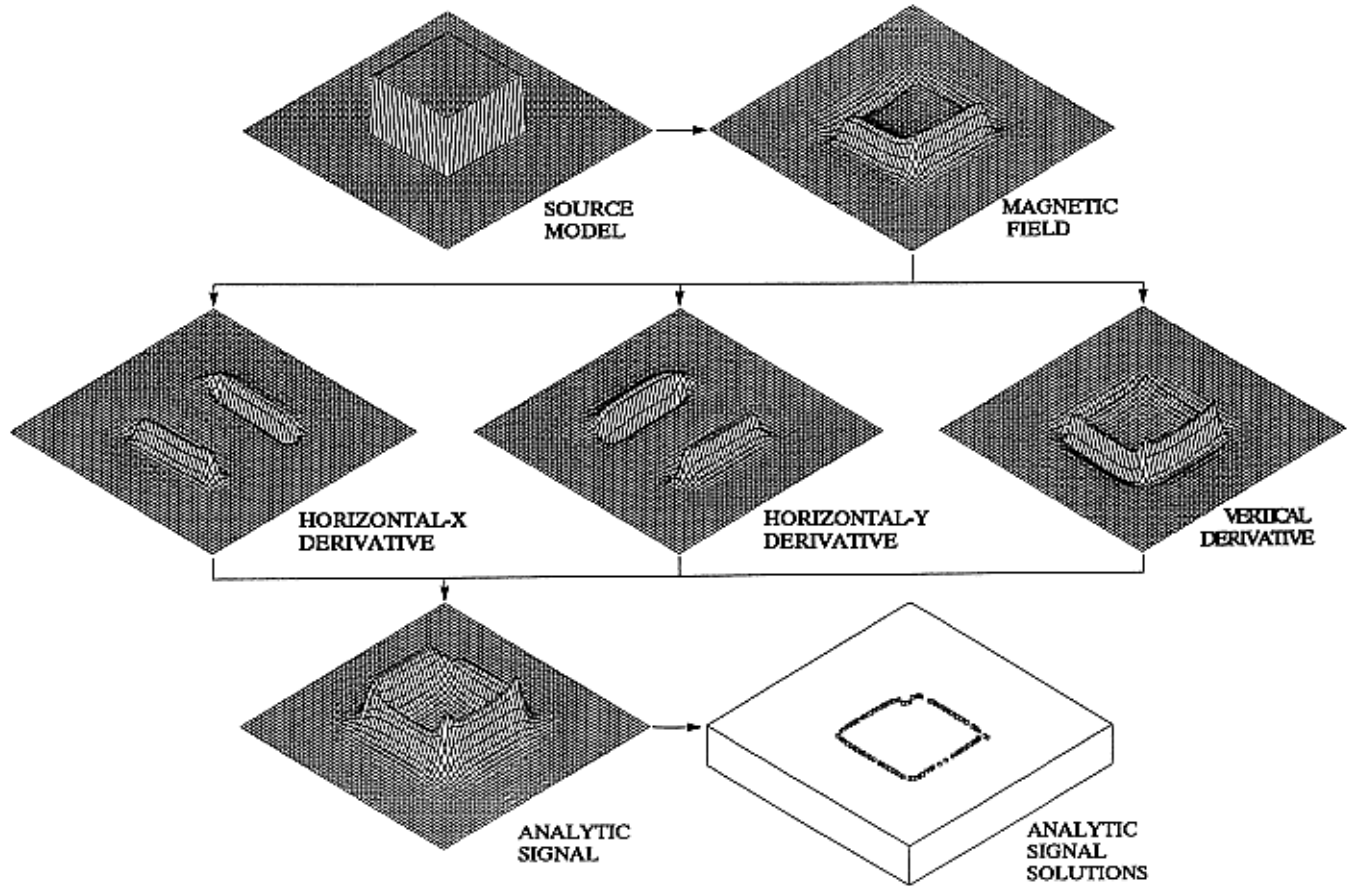


FIG. 1. Schematic outline of the analytic signal method. Horizontal and vertical derivatives are calculated from the total field anomaly over a square prism and combined to yield the absolute value of the analytic signal. The locations of the maxima and the shape of this signal can then be used to find body edges and corresponding depth estimates.

the characteristics of the source of the magnetic anomalies. However, due to the amplitude factor C_p (e.g., Schouten, 1971), the amplitude of the analytic signal varies with the strike of a 2-D body in the same way as does the amplitude of a magnetic anomaly. For example, as a result of this geometric amplitude factor, north-south trending sea floor spreading anomalies near the equator are very weak. It is possible to correct for this amplitude variation by reducing the observed anomalies to the pole. However, this would greatly reduce the power of the method, because one would have to introduce the direction of source body magnetization, which is often not known. Consequently, variations in the amplitude of the analytic signal should be interpreted with caution. Therefore, we will mainly use the shape of the absolute value of the analytic signal as an interpretational aid.

Nabighian (1972) calculated the shape of the analytic signal over several simple bodies. In this study we use the analytic signal over a vertical magnetic contrast at depth d , given by:

$$|A(x)| \propto \frac{1}{x^2 + d^2}. \quad (12)$$

Equation (12) shows that the amplitude of the analytic signal has a bell shape, with a half width that equals the depth to the magnetic source. If the magnetic contrast occurs in a layer with significant thickness, the resulting depth to source will be located between the top and the bottom of the layer. The larger the distance between top and bottom of the layer, relative to the level of observation, the more the result tends to converge towards the top of the layer.

The absolute value of the analytic signal is often referred to as the energy envelope of a signal (cf. Oppenheim and Schaffer, 1975, p. 361). To illustrate this, Figure 2 shows that the absolute value of the analytic signal is the envelope of all possible phase shifts of an observed anomaly. In this case we calculated an anomaly over a vertical magnetization contrast. It is easily recognized that the shape of this envelope is independent of the skewness of the observed profile, because the total range (360 degrees) of the phase shift parameter is covered. The envelope has a maximum that is located directly above the magnetic contrast. However, the sign of the magnetic contrast is lost in the absolute value of the signal. Therefore, when using this technique one cannot determine whether a given source has a higher or lower susceptibility than its surroundings. The absolute value of the analytic signal in three dimensions is also the envelope over all possible directions of magnetization and inducing field. Graphically, this cannot be shown as easily as in the 2-D case. In addition, demonstration would involve a large number of calculations, because one would have to vary four parameters, i.e., the inclinations and declinations of the earth's magnetic field and of the source body magnetization.

APPLICATIONS

Several applications of the analytic signal, and of the complex gradient, of magnetic anomalies along profiles have been published (Nabighian, 1972, 1974; Atchuta Rao et al., 1981; Thompson, 1982; Nelson, 1988b). However, only limited work has been published on the practical use of the

3-D analytic signal introduced by Nabighian (1984). Hansen et al. (1987) used the 3-D analytic signal in the interpretation of gravity data. Here we develop a practical method to derive the positions of magnetic contrasts and their depth from the amplitude of the analytic signal of gridded data.

Maxima in the analytic signal indicate positions of magnetic contrasts. A simple method for the automated detection of these maxima is based on Blakely and Simpson's (1986) approach for pseudo gravity anomalies. The procedure finds the location of maxima of a field defined at a regular grid by comparing the value at a central grid location in a 3×3 grid window with that of its four pairs of surrounding grid points (Figure 3). A parabola is fitted through each of the four sets of three points. A maximum for this parabola is accepted if it is located inside the central grid cell (square box in Figure 3), and if its value exceeds that of the outer two points. In case several triplets reach a valid maximum, we used the location and value of the highest maximum. After obtaining the location of this maximum, several criteria can be applied to qualify it. Blakely and Simpson (1986) used the value of the maximum and an index N , which they defined as the number of valid maxima found in the 3×3 window. This index N gives an indication of the linearity of a maximum: If N is 1, the anomaly is linear, but tilted; if N is 4, the maximum is a local peak. Blakely and Simpson (1986) found that, in general, indices 2 and 3 were most useful. Maps made with index 1 showed, for example, maxima that radiate from circular features in directions that depend on the grid orientation. To suppress this type of maximum, we added the value of the curvature, or second

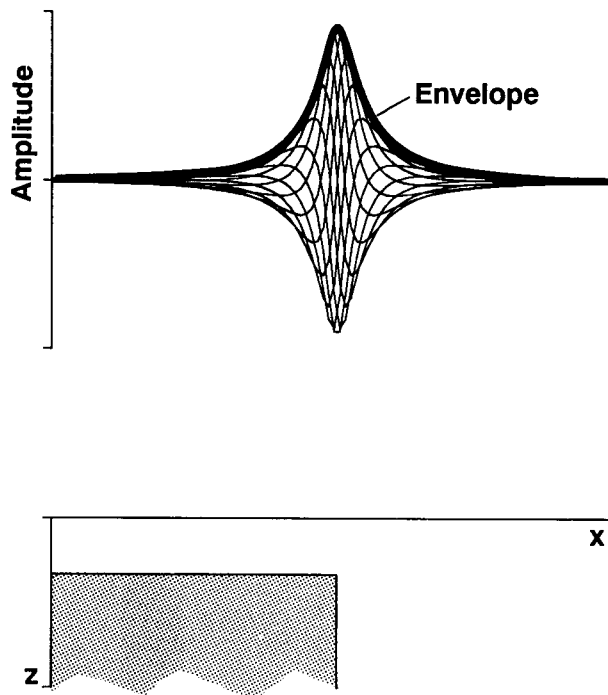


FIG. 2. The absolute value of the analytic signal is known as the energy envelope. This envelope can be obtained by phase shifting of an anomaly, in this case over a magnetic contrast, over a range of 360 degrees. The individual curves inside the envelope represent the anomaly shifted in steps of 30 degrees.

derivative, at the location of the maximum as a third criterion for selection of maxima. The selection based on curvature proved useful to eliminate certain unwanted maxima without affecting others that were of interest.

Once maxima in the amplitude of the analytic signal have been accepted, the depth to the magnetic source bodies can be estimated from the shape of the analytic signal. The use of the half width of the bell-shaped function over a simple contrast, given by equation (14), was suggested by Nabighian (1972, 1974) and more detailed calculations were presented by Atchuta Rao et al. (1981). However, to determine the shape of the analytic signal over each maximum, one needs to first establish the strike of the linear magnetic anomaly. Although a number of methods can be used to obtain this strike, an algorithm that finds the azimuth with the narrowest cross-section was found to be very reliable. This narrowest cross-section, extracted from the gridded values, is then assumed to be perpendicular to the strike. After that, a bell-shaped function [equation (14)] is fitted to this cross-section and its half width provides an estimate of the depth to the contrast. If this fit is poor, in terms of rms misfit between amplitude of analytic signal and best fitting bell-shaped curve, the depth estimate can be rejected. A poor fit may be an indication of interference of multiple anomalies. In addition, as mentioned above, one can select only a certain class of maxima based on the value of the maximum, the index N , and the second derivative at the location of the maximum.

Because peaks in the analytic signals over two contrasts, with a spacing less than their depths, merge to one (Atchuta Rao, 1981), caution is needed when source depths are calculated from the analytic signal. The effect of interfering anomalies on the depth estimates can be reduced by estimating depths from the width at 60 percent to 80 percent of the amplitude, rather than from the half width. However, if the

grid spacing is too wide, not enough grid points may be available to give reliable results.

Figure 4a shows a model anomaly over some irregularly shaped prisms calculated on a grid 70×70 grid cells in size. The locations of maxima in the analytic signal calculated from this anomaly are the centers of the circles in Figure 4b. Superimposed are the outlines of the source bodies and the depths to their tops in arbitrary units equal to the grid interval. The bottom of the model is constant at five units. It is clear that in this case the analytic signal helps to outline the geometry of the sources, especially that of the smallest body. The right-hand side of this latter body is mislocated because its strike is almost parallel to the magnetic field. As a result the amplitude factor and, consequently, the magnetic anomaly over this edge are very small (Figure 4a). In Figure 4b, the depth estimates obtained from the shape of the analytic signal are indicated by the size of the symbol; the deeper the source, the larger the radius of the circle. Comparison with the model bodies shows that the obtained estimates are reasonably accurate. The largest deviations occur where the source geometry is not 2-D and where the edges of different bodies are close together.

EXAMPLES

Lake Huron

Figure 5a shows magnetic field intensity data from a $168 \times 168 \text{ km}^2$ area centered on southern Lake Huron at the border between Canada and the United States. The data comprise several surveys of different quality from both the United States and Canada that were leveled and merged at the Geological Survey of Canada. The area is dominated by the northeast-southwest trending high ($>300 \text{ nT}$) associated with the Grenville front that separates the Grenville Province to the southeast from the Superior Province to the northwest. A general increase in field complexity is apparent in a south-easterly direction.

No crystalline basement outcrops are present in the study area, which is overlain by post-Ordovician sediments that generally thicken towards the west. Structure within the basement is suspected to strongly influence the location of faulting within the Paleozoic cover that is associated with known oil and gas occurrences (Sanford et al., 1985). The basement geology is constrained by drill hole data and, in conjunction with aeromagnetic and gravity data, can be divided into several lithotectonic domains (Carter and Easton, 1990). To the southeast of the Grenville Front, the study area lies inside the Huron domain that is characterized by quartzofeldspathic rocks ranging from granitic to tonalitic in composition. Some rocks are also gneissic in character (Turek and Robinson, 1982). Lithological variations in the Precambrian basement are emphasized on the analytic signal map (Figure 5b). In particular, at the southern tip of Lake Huron, a major circular feature (C in Figure 5b) can be seen that has been identified as a possible impact crater (Forsyth et al., 1990). Conformable arcuate trends are apparent out to distances of 100 km from the center of the structure.

Data quality and consistency are important factors in determining the effectiveness of the depth estimates from the 3-D analytic signal approach. Artifacts arising from variations in flight line spacing and/or leveling errors are accen-

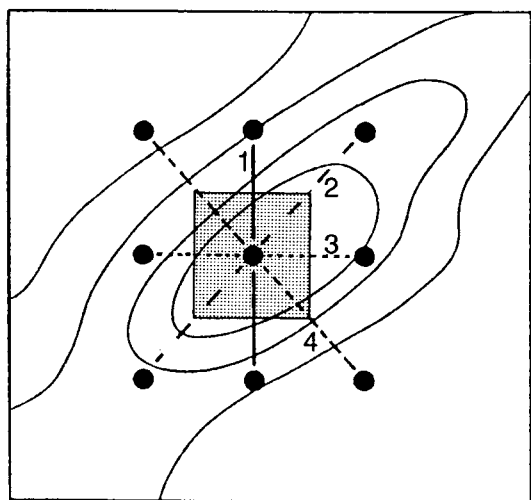


FIG. 3. Determination of maxima from grid values in a 3×3 window (after Blakely and Simpson, 1986). A parabola is fitted through each of the four triplets indicated. The number of parabolas that reach a maximum inside the center grid cell (box) gives the index N ($1 \leq N \leq 4$). If N exceeds 1, the value and location of the highest maximum is used.

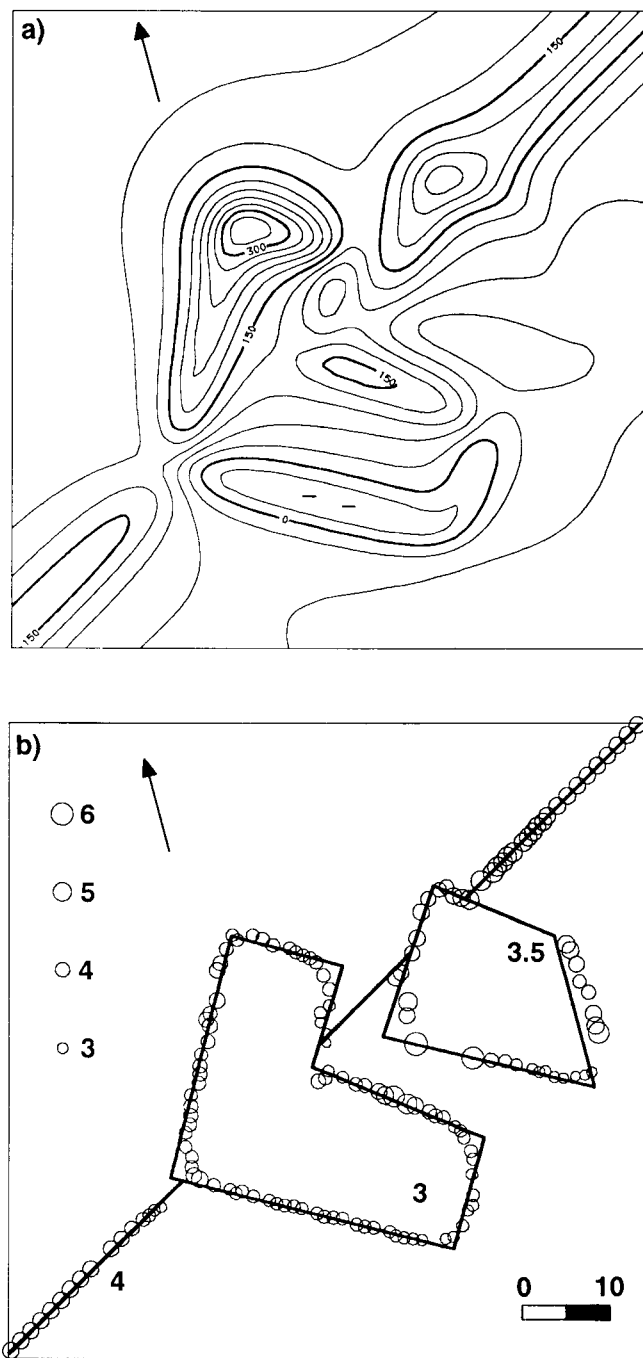


FIG. 4. (a) Synthetic magnetic anomaly over irregularly shaped prisms with a magnetization contrast of 3 A/m, assuming an inducing field with inclination -33 degrees and declination -20 degrees (indicated by the arrow). (b) Locations of the maxima in the analytic signal, with their corresponding depth estimates indicated by the size of the circles. Superimposed are the body outlines with their depths to the top indicated in arbitrary units that are equal to the grid interval. The bottoms are fixed at five units. Horizontal scale is in grid cell units.

tuated by the analytic signal since we are dealing with a combination of spatial derivatives, all of which magnify the high-frequency content of the data. Corrugation effects due to the above sources can be seen in Figure 5b; in a north-south direction in the central west and with an east-west trend in the northwest of the study area. Groupings of corresponding depth estimates (Figure 5c) are readily apparent.

Analytic signal depth estimates of the western rim of the circular feature beneath southern Lake Huron show depths of 3-4 km, in agreement with results from Euler deconvolution (Forsyth et al., 1990). The eastern edge of the structure, which is not very well resolved, appears slightly shallower, with depth values of 2-3 km. Borehole data suggest a maximum of 2 km of Paleozoic sediments in this area, thus indicating a Precambrian age for the structure. The study area on the whole shows a distinct change in character from the southeast, where solutions are generally shallow (1-5 km), to the northwest where depth to source estimates are consistently deeper (4-15 km). This change in both the pattern and source depths, which is approximately parallel to the U.S.-Canada border (Figure 5c), is not related to survey boundaries, but most likely represents a change in structural style between the Superior and Grenville Provinces. Thus, the magnetic source distribution suggests a Grenville front position about 80 km to the southeast of that predicted by Forsyth et al. (1990, 1 in Figure 5c) from an extrapolation of the front identified from seismic reflection data (Green et al., 1988). This difference can be accounted for by assuming a slightly different trend for the Grenville front between the study area and the seismic line, the latter being located about 200 km farther north.

Sydney Basin

The second example illustrates the use of the analytic signal for the detection of geological boundaries in the Northern Appalachian Orogen. Recently, the continuation of terranes from Cape Breton Island to Newfoundland in eastern Canada was studied by Loncarevic et al. (1989), using geophysical data. Several tectono-stratigraphic terranes have been identified in Cape Breton and Newfoundland (cf. Williams and Hatcher, 1983; Barr and Reaside, 1989), and deep seismic reflection profiles relate them to deeper crustal blocks (Marillier et al., 1989). However, no ground truth evidence exists for the correlation of terranes on either side of the Cabot Strait.

Loncarevic et al. (1989) used the horizontal derivative of the vertical magnetic gradient to define terrane boundaries in this area. They reduced anomalies to the pole and assumed induced magnetization. The analytic signal technique could contribute here, because no assumption with regard to the magnetization is required. Figure 6 shows the locations of maxima in the analytic signal. The continuation of boundaries between the Notre Dame, Aspy, and Bras d'Or terranes (Barr and Reaside, 1989) are recognized (A and B in Figure 6). Their trends are slightly different from those derived by Loncarevic et al. (1989). However, in the deeper part of the Sydney basin, no consistent trends were found. Inspection of the horizontal derivative (Loncarevic et al., 1989) reveals that the boundary between Bras d'Or and

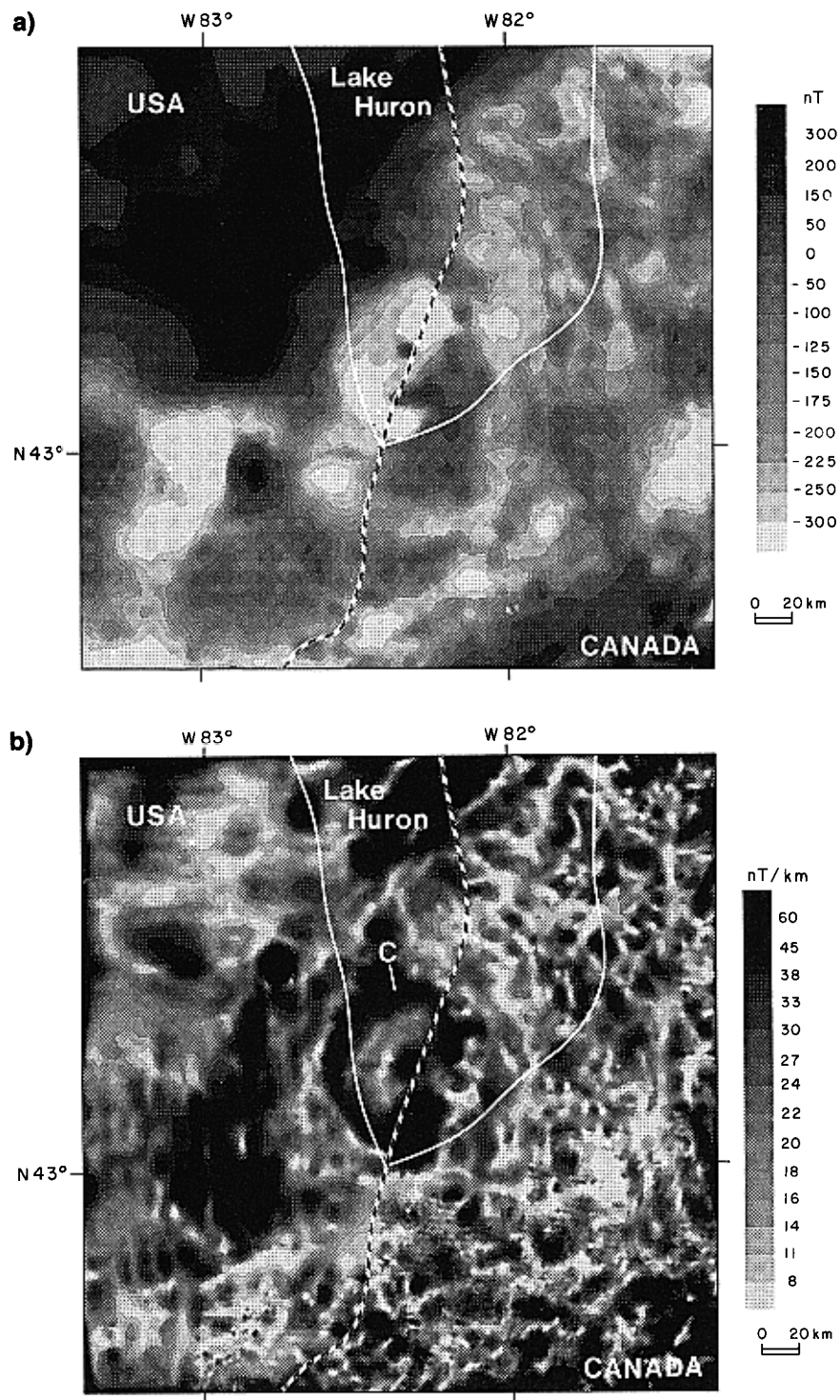


FIG. 5. (a) Observed total field magnetic anomaly over Lake Huron. The area comprises 420×420 grid cells with a grid interval of 400 m. The border between Canada and the United States is indicated by the dashed line. (b) The analytic signal calculated from this anomaly displays a circular feature in the center of the image, marked (C). The eastern half of this feature is less well developed. (c) Locations of the maxima in the analytic signal, with their corresponding depth estimates with respect to the level of observation (300 m). The larger the circles, the deeper the underlying sources. Also indicated are the approximate locations of the Grenville front, separating the Grenville Province in the southeast from the Superior Province in the northwest, as proposed previously (labeled 1 in Figure 5c) and in this study (labeled 2).

Avalon terranes (C in Figure 6) is indeed less evident. In an effort to improve resolution, we also calculated the analytic signal of the first vertical derivative of the magnetic anomalies (cf. Nabighian, 1974). However, because the grid consists of combined data sets with different quality (see Loncarevic et al., 1989), seams and other artifacts resulting from the gridding procedure as well as track corrugations appeared, which made a sensible interpretation of this map impossible.

The analytic signal was also used to derive depth estimates. The deepening of the basement in the Sydney basin is clearly visible, as well as the shallow solutions onshore. The boundary between the Notre Dame and Aspy terranes is located at a rather constant depth of about 3.5 to 4 km. The depth estimates show similar general trends as shown on a map derived from interactive modeling of individual anomalies in the area (B. D. Loncarevic, pers. comm.). In addition, they seem to be in reasonable agreement with deep seismic reflection line 86-5A (Marillier et al., 1989).

DISCUSSION AND CONCLUSION

The examples given above show the potential of the analytic signal of magnetic anomalies for geophysical interpretation. As we have demonstrated, the shape of the absolute value of the analytic signal over 2-D source bodies is independent of the direction of source body magnetization and the direction of the Earth's field. The generalization of the analytic signal method to three dimensions is an improvement that allows for the analysis of much larger

volumes of data. In addition, the restrictive assumption of two-dimensionality is relaxed. Nevertheless, the data should be interpreted with care. First, the amplitude of the analytic signal varies with the effective magnetization, and therefore remains a function of the ambient magnetic field parameters. This will, for example, lead to problems when interpreting the analytic signal close to the magnetic equator. Second, the analytic signal over magnetization contrasts that are closely spaced or dipping are more complicated than the assumed bell-shaped function found over a single contrast. Since we take the absolute value of the signal, the process is not linear and the results cannot be deconvolved into a set of curves resulting from simple steps. Third, the analytic signal over structures that intersect at an acute angle is complicated because of the nonlinear combination of signals. And finally, as the calculation of the analytic signal is based on derivatives of the magnetic anomalies, gridding artifacts, errors like track corrugations, and noise in general, are all enhanced.

Recently, the 3-D generalization of the 2-D Euler deconvolution (Thompson, 1982) was developed by Reid et al. (1990). A preliminary comparison of this method with the analytic signal (Pilkington et al., 1990) shows a reasonable agreement of their solutions. However, the number of solutions found in both methods is different. Each grid cell in a gridded data set can only give one solution using the analytic signal. However, using the Euler deconvolution one may find a whole suite of solutions, both horizontally and vertically displaced with respect to the grid cell under consider-

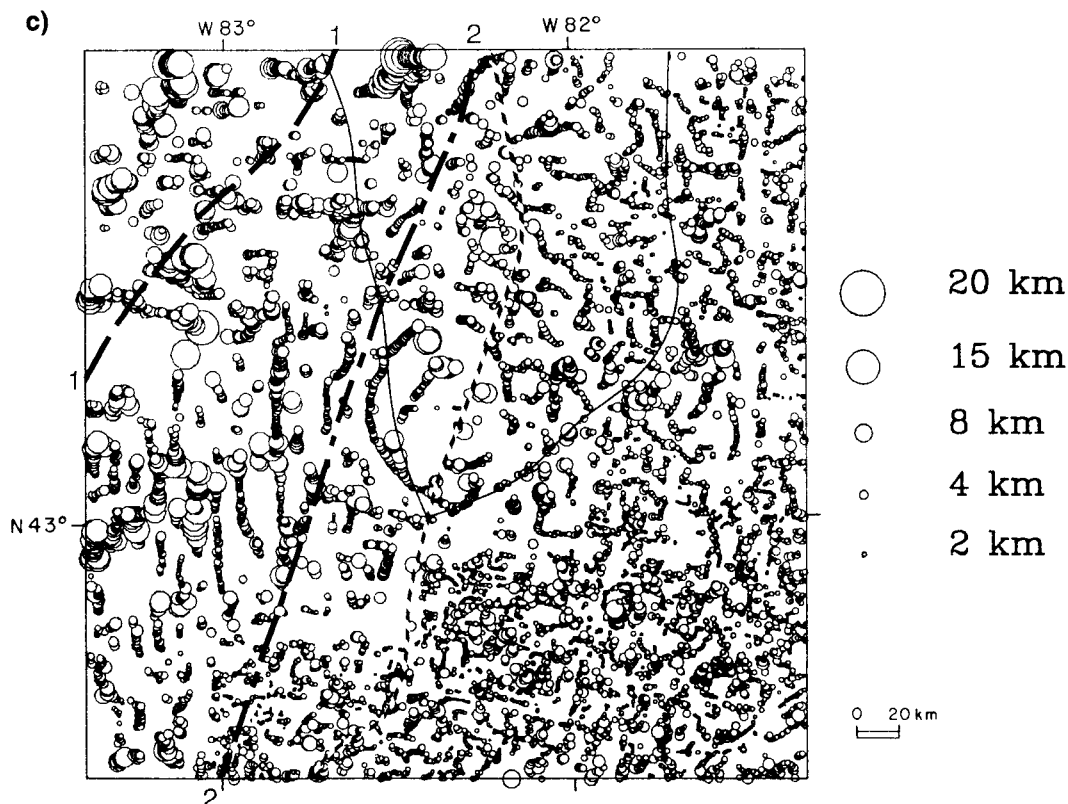


FIG. 5. continued

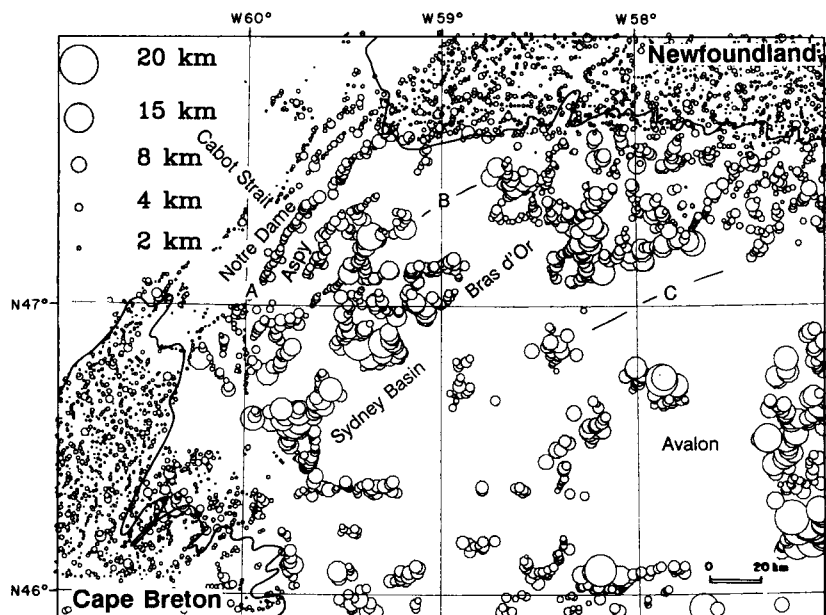


FIG. 6. Locations of magnetic contrasts and depth estimates obtained from aeromagnetic data over Cape Breton, Newfoundland and the Sydney Basin. The magnetic grid has a spacing of 812.8 m, and contains 590×435 grid cells. The flight elevation was 300 m. Line A indicates the proposed boundary between the Notre Dame and Aspy terranes, B the boundary between the Aspy and Bras d'Or terranes. Boundary C, between the Avalon and Bras d'Or terranes, is not well recognized.

ation. This makes visualization and interpretation of 3-D Euler solutions very difficult. In addition, the user defined structural index used in the Euler deconvolution is very critical, not only for the depth estimates obtained, but also for their locations. We conclude that a combination of both methods may be most useful, where the analytic signal can be used to outline magnetic contrasts, and their approximate depths, and the Euler deconvolution can give a more detailed structural interpretation at depth.

There are a number of ways to improve the practical application of the analytic signal. For example, if the interference from adjacent bodies is not present, it is possible to determine the signature of the causative body of the magnetic anomaly from the exact shape of the analytic signal. Essentially, this involves determination of the power of the denominator of Equation (14), which was set equal to 1 in our applications.

Furthermore, to facilitate the selection of solutions, an interactive graphical method will be developed that allows browsing through all solutions in a 3-D projection, without a priori selection. Thresholds for the various selection criteria can then be set interactively, and by comparison with geological models. This method can also prove valuable in the interpretation of solutions of other 3-D methods, like Euler deconvolution. Finally, the application of the analytic signal does not have to be restricted to magnetic anomalies, but it can also be applied to gravity (see for instance Hansen et al., 1987), or a combined analysis of potential field data.

ACKNOWLEDGMENTS

We thank Pierre Keating and John Broome for their critical reviews and an anonymous reviewer for his thoughtful comments. Geological Survey of Canada Contribution, No. 54590.

REFERENCES

- Atchuta Rao, D., Ram Babu, H. V., and Sanker Narayan P. V., 1981, Interpretation of magnetic anomalies due to dikes: The complex gradient method: *Geophysics*, **46**, 1572–1578.
- Barr, S. M., and Reaside, 1989, Tectono-stratigraphic terranes in Cape Breton Island, Nova Scotia: Implications for the configuration of the northern Appalachian Orogen: *Geology*, **17**, 822–825.
- Blakely, R. J., and Simpson, R. W., 1986, Approximating edges of source bodies from magnetic or gravity anomalies: *Geophysics*, **51**, 1494–1498.
- Carter, T. R., and Easton, R. M., 1990, Extension of Grenville basement beneath southwestern Ontario: Lithology and tectonic subdivisions, in Carter, T. R., Ed., *Subsurface geology of Southwestern Ontario: A core workshop*: Ontario Petroleum Institute, Am. Assn. Petr. Geol. 1990 East. Sec. Mtg., 9–28.
- Committee for the Magnetic Map of North America, 1988, *Magnetic anomaly map of North America: The Leading Edge*, **7**, 19–21.
- Dods, S. D., Teskey, D. J., and Hood, P. J., 1985, The new series of 1:1 000 000-scale magnetic anomaly maps of the Geological Survey of Canada: *Compilation techniques and interpretation*, in Hinze, W. J., Ed., *The utility of regional gravity and magnetic anomaly maps*: Soc. Expl. Geophys., 69–87.
- Forsyth, D. A., Pilkington M., Grieve, R. A. F., and Abinett, D., 1990, A major circular structure beneath southern Lake Huron from potential field data: *Geology*, **18**, 773–777.
- Green, A. G., Milkereit, B., Davidson, A., Spencer, C., Hutchinson, D. R., Cannon, W. F., Lee, M. W., Agena, W. F., Be-

- hrendt, J. C., and Hinze, W. J., 1988, Crustal structure of the Grenville front and adjacent terranes: *Geology*, **16**, 788–792.
- Hansen, R. O., Pawlowski, R. S., and Wang, X., 1987, Joint use of analytic signal and amplitude of horizontal gradient maxima for three-dimensional gravity data interpretation: 57th Ann. Internat. Mtg., Soc. Expl. Geophys., Expanded Abstracts, 100–102.
- Loncarevic, B. D., Barr, S. M., Reaside, R. P., Keen C. E., and Marillier, F., 1989, Northeastern extension and crustal expression of terranes from Cape Breton Island, Nova Scotia, based on geophysical data: *Can. J. Earth Sci.*, **26**, 2255–2267.
- Marillier, F., Keen, C. E., Stockmal, G. S., Quinland, G., Williams, H., Colman-Sadd, S. P., and O'Brien, S. J., 1989, Crustal structure and surface zonation of the Canadian Appalachians: Implications of deep seismic reflection data: *Can. J. Earth Sci.*, **26**, 305–321.
- Nabighian, M. N., 1972, The analytic signal of two-dimensional magnetic bodies with polygonal cross-section: Its properties and use for automated anomaly interpretation: *Geophysics*, **37**, 507–517.
- 1974, Additional comments on the analytic signal of two-dimensional magnetic bodies with polygonal cross-section: *Geophysics*, **39**, 85–92.
- 1984, Toward a three-dimensional automatic interpretation of potential field data via generalized Hilbert transforms: Fundamental relations: *Geophysics*, **49**, 780–786.
- Nelson, J. B., 1988a, Calculation of the magnetic gradient tensor from total field gradient measurements and its application to geophysical interpretation: *Geophysics*, **53**, 957–966.
- 1988b, Comparison of gradient analysis techniques for linear two-dimensional magnetic sources: *Geophysics*, **53**, 1088–1095.
- Ofoegbu, C. O., and Mohan, N. L., 1990, Interpretation of aeromagnetic anomalies over part of southeastern Nigeria using three-dimensional Hilbert transformation: *Pageoph.*, **134**, 13–29.
- Oppenheim, A. V., and Schaffer R. W., 1975, *Digital signal processing*: Prentice-Hall Inc.
- Pedersen, L. B., 1989, Relations between horizontal and vertical gradients of potential fields: *Geophysics*, **54**, 662–663.
- Pilkington, M., Roest, W. R., and Verhoef, J., 1990, Automated depth estimation from gridded potential field data [abstract]: *EOS, Trans. Amer. Geophys. Un.*, **71**, 1643.
- Reid, A. B., Allsop, J. M., Granser, H., Millett, A. J., and Somerton, I. W., 1990, Magnetic interpretation in three dimensions using Euler deconvolution: *Geophysics*, **55**, 80–91.
- Schouten, J. A., 1971, A fundamental analysis of magnetic anomalies over ocean ridges: *Mar. Geophys. Res.*, **1**, 111–144.
- Sanford, B. V., Thompson, F. J., and McFall, G. H., 1985, Plate tectonics—a possible controlling mechanism in the development of hydrocarbon traps in southwestern Ontario: *Bull. Can. Petr. Geol.*, **33**, 52–71.
- Thompson, D. T., 1982, EULDPH: A new technique for making computer-assisted depth estimates from magnetic data: *Geophysics*, **47**, 31–37.
- Turek, A., and Robinson, R. N., 1982, Geology and age of the Precambrian basement in the Windsor, Chatham, and Sarnia areas, southwestern Ontario: *Can. J. Earth Sci.*, **19**, 1627–1634.
- Wang, X., and Hansen, R. O., 1990, Inversion for magnetic anomalies of arbitrary three-dimensional bodies: *Geophysics*, **55**, 1321–1326.
- Williams, H., and Hatcher, R. D., 1983, Appalachian suspect terranes, in *Contributions to the tectonics and geophysics of mountain chains*, Hatcher, R. D., Williams, H., and Zietz, I., Eds.: *Geol. Soc. Am., Memoir* **158**, 33–53.